BIODIVERSITAS
Volume 27, Number 1, January 2026
Pages: 16

ISSN: 1412-033X
E-ISSN: 2085-4722
https://doi.org/10.13057/biodiv/d270135

Fertilization strategies alter growth and rhizosphere microbiome diversity in white potato (*Solanum tuberosum*)

ALUH NIKMATULLAH[1,♥], MUHAMMAD SARJAN[1], AMRUL JIHADI[1], IHLANA NAIRFANA[2], EKA SUNARWIDHI PRASEDYA[3]

[1]Faculty of Agriculture, Universitas Mataram. Jl. Majapahit 62, Mataram 83127, West Nusa Tenggara, Indonesia. Tel./fax.: +62-271-663375, [♥]email: aluh_nikmatullah@unram.ac.id

[2]Department of Food Technology, Faculty of Agricultural Technology, Universitas Teknologi Sumbawa. Jl. Raya Olat Maras, Sumbawa 84371, West Nusa Tenggara, Indonesia

[3]Department of Biology, Faculty of Mathematics and Natural Sciences, Universitas Mataram. Jl. Majapahit 62, Mataram 83127, West Nusa Tenggara, Indonesia

Manuscript received: 30 August 2025. Revision accepted: 26 January 2026.

Abstract. *Nikmatullah A, Sarjan M, Jihadi A, Nairfana I, Prasedya ES. 2026. Fertilization strategies alter growth and rhizosphere microbiome diversity in white potato (*Solanum tuberosum*). Biodiversitas 27 (1): d270135. https://doi.org/10.13057/biodiv/d270135.* Excessive inorganic fertilization is widely used to boost potato productivity, but often reduces nutrient-use efficiency and disrupts soil microbial communities. This study evaluated how three fertilization regimes viz. CF100 (100% recommended inorganic + organic fertilizer), CF50 (50% recommended inorganic + organic fertilizer), and CF50OF (50% recommended inorganic + organic fertilizer + biofertilizer), affect plant growth, yield, and rhizosphere microbiome composition of white potato (*Solanum tuberosum*). Growth assessments at five weeks after shoot emergence showed that CF50OF produced significantly higher shoot numbers, fresh biomass, and dry biomass compared to CF50, and achieved growth comparable to CF100. Tuber yield did not differ significantly among treatments. Amplicon sequencing of rhizosphere soil revealed that fertilization strategy strongly shaped microbial richness, taxonomic composition, and phylogenetic structure. CF100 exhibited the highest observed taxa and phylogenetic diversity, whereas CF50OF enriched a broader spectrum of low-abundance and functionally diverse microbial genera associated with nutrient cycling, organic matter degradation, hormone production, biocontrol, abiotic stress adapters, and other functions. Despite lower Shannon and Simpson diversity values compared to CF100 and CF50, CF50OF supported microbial communities with greater functional potential, which may compensate for reduced inorganic inputs. These findings demonstrate that integrating biofertilizer with reduced inorganic fertilizer can sustain potato growth while promoting a more ecologically functional rhizosphere microbiome, offering a promising strategy for nutrient-efficient and environmentally sustainable potato cultivation.

Keywords: Biofertilizer, ecological resilience, integrated fertilization management, microbial diversity, sustainable agriculture

INTRODUCTION

Potato (*Solanum tuberosum* L.) is the fourth most important food crop globally after rice, wheat, and maize (Jennings et al. 2020). Cultivated in over 150 countries, its global harvested area reached 18.1 million hectares in 2021 (FAO 2023). Asia accounts for more than half of global production areas, though Southeast Asia contributes less than 1% (FAO 2023). In tropical regions like Indonesia, potatoes thrived in highland areas with cooler temperatures and well-drained soils (Gunadi and Pronk 2023; Buckseth et al. 2024). The crop is cultivated in half of Indonesia's Provinces, with annual production ranging from 1.2 to 1.3 million tons over the past five years (BPS 2025). However, domestic production has not kept pace with rising demand; driven by population growth, changing dietary preferences, and rapid expansion of the food industry, leading to an increase in imports, from 48,952 tons in 2017 to 80,345 tons in 2021 (FAO 2023).

Potato productivity in tropical regions remains below the global average, with yields of approximately 17.5 tons/ha compared to 20.7 tons/ha worldwide (FAO 2023). To boost yields, growers often rely on intensive inorganic fertilization, as potatoes respond strongly to nutrient inputs (Lombardo et al. 2020; Yadav et al. 2024). In Indonesia, fertilization rates vary by region and soil conditions, typically ranging from 200-400 kg N ha^{-1}, 200-300 kg P ha^{-1}, and 250-350 kg K ha^{-1}, often supplemented with organic fertilizer. For example, West Java report rates of 394 kg N ha^{-1}, 249 kg P ha^{-1}, and 313 kg K ha^{-1} (Pronk et al. 2025), while West Nusa Tenggara applies 385 kg N ha^{-1}, 220 kg P ha^{-1}, and 320 kg K ha^{-1} (Nurhidayah et al. 2023). These high inputs aim to maximize yield but raise concerns about nutrient inefficiency and environmental degradation.

Potatoes exhibit relatively low nutrient uptake efficiency, with nitrogen (N) utilization ranging from 40-50% (Makani et al. 2020; Tiwari et al. 2020), and phosphorus (P) uptake often lower (Kirchgesser et al. 2020; Chea et al. 2024). Excessive nitrogen fertilization does not always boost potato yield; it often promotes excessive vegetative growth at the expense of tuber development, leading to reduced productivity (Fang et al. 2024; Ren et al. 2025). Optimizing fertilization dosage is critical to improve nutrient use efficiency, enhance economic returns, and reduce environmental risks (Wang et al. 2024; Chabani et al. 2025;

Gao et al. 2025). Excess nitrogen can lead to nitrate accumulation, contributing to soil acidification, water contamination, greenhouse gas emissions, biodiversity loss, and soil salinization (Betancur Corredor et al. 2022; Wang et al. 2022).

Hence, to address these challenges of conventional fertilization and support Sustainable Development Goals, integrated fertilization strategies, combining chemical, organic, and biological inputs, are gaining increased attention. The use of mineral fertilizers alongside organic and biofertilizer amendments can reduce reliance on inorganic inputs while sustaining crop productivity. Organic compost, especially manure-based, improves soil fertility (Ji et al. 2020a); however, it may introduce soil-borne pathogens (Xu et al. 2022) and alter the native microbial community dynamics (Ji et al. 2020b). In contrast, biofertilizers containing beneficial microorganisms offer a promising solution to mitigate these risks, suppress pathogens, and enhance plant growth. Previous studies demonstrated that biofertilizers modulate the soil and rhizosphere microbiome, enhancing microbial diversity and enriching beneficial microbes (Liu et al. 2022; Raman et al. 2022; Ng et al. 2025). Despite promising results, few studies have systematically explored how integrated fertilization strategies affect potato growth, rhizosphere microbiome composition, and agronomic performance. This gap limits the development of fertilization regimes that balance productivity and ecological health.

Therefore, to address this, the present study evaluates the impact of three fertilization regimes: CF100 (100% inorganic + organic fertilizer), CF50 (50% inorganic + organic fertilizer), and CF50OF (50% inorganic + organic fertilizer + biofertilizer) on the growth, yield, and rhizosphere microbiome diversity of white potato. By integrating agronomic performance metrics with microbial profiling, we assess whether reduced mineral input, supplemented with organic and biological amendments, can sustain productivity while fostering a healthier soil microbiome. We hypothesize that integrating biofertilizer with reduced inorganic fertilizer (CF50OF) will sustain potato growth and biomass production at levels comparable to full inorganic fertilization (CF100) by enriching functionally important rhizosphere microbial taxa—such as nutrient cyclers, organic matter degraders, and plant growth-promoting bacteria—thereby enhancing nutrient availability and ecological resilience despite lower chemical input.

MATERIALS AND METHODS

Experimental site and growth conditions

The experiment was conducted in a screen house at the experimental site in Sembalun Village (8°21'18.5"S, 116°31'00.7"E), Sembalun District, West Nusa Tenggara, Indonesia, situated at approximately 1,100 m above sea level. The site experiences a subtropical highland climate, with minimum and maximum temperatures of 18.6 and 29.2°C, respectively, and an average monthly rainfall of 41.5 mm during the experimental period (15 July to 15 October 2024).

Experimental design

The experiment followed a randomized complete block design (RCBD) with three fertilization treatments and five replicates (blocks) per treatment (Table 1). Five blocks were arranged along the sunlight gradient, from the morning-light-exposed side to the afternoon-light-exposed side, and treatments were randomly assigned within each block. Each treatment was implemented in two series: the first series was designated for destructive sampling at five weeks after planting to assess early physiological and microbial parameters, while the second series was maintained until harvest for yield analysis. Plants were arranged with a spacing of 40 cm between polybags within each block and 50 cm between blocks, allowing sufficient room for plant growth, sampling activities, and minimizing inter-block interference. Potato plants were cultivated in 14.6 L polybags (26 cm diameter × 28 cm height) containing 11 kg of growth media under screen house conditions, with each fertilization treatment applied as per the experimental design. Each polybag was placed on an individual plastic tray (diameter 5 cm, height 4 cm) to prevent runoff and cross-contamination, thereby maintaining optimal soil moisture and treatment independence.

Fertilization composition and application

The inorganic fertilizer regime was based on local agronomic recommendations used by potato farmers in Sembalun. The full-dose mixture (CF100) consisted of: 650 kg ha^{-1} of commercial NPK (16:16:16), 300 kg ha^{-1} of superphosphate (SP-36), 300 kg ha^{-1} of potassium chloride (KCl), and 300 kg ha^{-1} ammonium sulfate (ZA). This corresponds to a nutrient input of 177.5 kg ha^{-1} nitrogen (N), 212 kg ha^{-1} diphosphorus pentoxide (P_2O_5), 290 kg ha^{-1} potassium oxide (K_2O), and 84 kg ha^{-1} sulfur (S), equivalent to 4.2 g N, 5.0 g P_2O_5, 6.9 g K_2O, and 2.0 g S per pot. Fertilizer application was split into two stages: pre-planting (½ dose of NPK + full dose of SP-36) and five weeks after shoot emergence (WAS) (½ dose of NPK + KCl + ZA). CF50 and CF50OF treatments received half the CF100 dosage.

Table 1. Summary of fertilization treatments used in the experimental design

Treatment code	Inorganic fertilizer	Organic fertilizer	Biofertilizer
CF100	100% recommended dose	¼ of the growth media volume	No
CF50	50% recommended dose	¼ of the growth media volume	No
CF50OF	50% recommended dose	¼ of the growth media volume	Yes

Organic fertilizer, comprising 25% of the total media volume (v/v), was uniformly applied across all treatments. The fertilizer consisted of fermented cow manure, prepared three weeks before planting. Dry cow dung was collected from the communal cowshed in Sembalun, sun-dried for three days with intermittent mixing to reduce moisture content, and subsequently fermented using a commercial fermentation solution for one week. Following manual homogenization, the fermentation solution was re-applied, and the mixture was allowed to ferment for an additional week. The final properties of the fermented manure were as follows: pH 7.67±0.01, total organic carbon 86,000±21 mg kg^{-1}, total nitrogen 7,100±14 mg kg^{-1}, total phosphorus 3,600±21 mg kg^{-1}, and a carbon-to-nitrogen (C/N) ratio of 23.4.

Biofertilizer was applied exclusively to the CF50OF treatment. The formulation contained: *Azospirillum* sp. (2.9×10^8 CFU/g), *Pseudomonas fluorescens* (2.9×10^9 CFU/g), and *Trichoderma asperellum* (2.5×10^7 propagules/g). The application concentration was prepared according to the manufacturer's instructions. One day before use, 100 g of biofertilizer was mixed with 1 L of water and incubated at room temperature for 24 hours. Just before application, the mixture was diluted 100-fold and applied at a rate of 200 mL per pot. The estimated CFU delivered per pot was approximately 5.8×10^6 for *Azospirillum* sp., 5.8×10^7 for *P. fluorescens*, and 5×10^5 propagules for *T. asperellum*. Biofertilizer was administered three times during the planting period: once on the day of shoot emergence, and subsequently at three and six weeks after shoot emergence (WAS).

Media preparation

The planting medium consisted of topsoil, fermented cow manure (organic fertilizer), and paddy husk charcoal mixed at a volumetric ratio of 2:1:1 (v/v/v). Topsoil was collected from the experimental site and sieved to remove rocks and plant debris. Its texture comprised 35% silt, 36% clay, and 29% sand. The chemical properties of the soil were as follows: pH 6.49±0.01, total organic carbon 19,800±14 mg kg^{-1}, total nitrogen 5,700±12 mg kg^{-1}, total phosphorus 210±11 mg kg^{-1}, total nitrogen 3,160±17 mg kg^{-1}, and available phosphorus 52.7±7.3 mg kg-1.

Plant maintenance

Potato plants were watered manually once daily in the morning using a hose fitted with a slow-release nozzle, allowing gradual watering until excess water drained from the polybag holes to maintain optimal soil moisture. The excess water was trapped in individual plastic trays placed beneath each polybag to prevent runoff and cross-contamination. Weeding was performed manually every week. To prevent pest and disease infestation, plants were sprayed at weekly intervals with Decis® 25 EC (2 mL/L) and Zampro® 525 SC according to recommended application rates.

Measurement of the growth and yield of potato

Plant growth was assessed at five weeks after shoot emergence (WAS), before the second fertilization. Non-destructive measurements included the number of compound leaves, canopy area, and the number of shoots per plant (de Jesus Colwell et al. 2021; Neilson et al. 2021; Chabani et al. 2025). The number of compound leaves was determined by counting fully expanded leaves (Chabani et al. 2025). Canopy area was calculated using a circular formula based on the average of three canopy diameter measurements: the widest, intermediate, and narrowest dimensions. The number of shoots was determined by counting the main stems emerging from each plant (Chabani et al. 2025). Fresh and dry biomass (de Jesus Colwell et al. 2021; Neilson et al. 2021; Khan et al. 2022; Hu et al. 2025) were measured destructively using the first series of samples. Fresh weight was recorded immediately using a triple beam balance (TBS2610S, Adam Co.) after carefully removing the plant from its polybag. To extract the plant, the polybag was cut open with a sharp blade, and soil was gently brushed from the roots using a paintbrush. This harvest was conducted following soil sampling for microbiome analysis. To assess plant dry weight, plant biomass was carefully trimmed, placed in labeled paper bags, and oven-dried at 70°C using a Memmert UN30 drying oven (Memmert GmbH + Co. KG, Schwabach, Germany). Drying was continued until a constant weight was achieved, and the dry weight was then measured using an analytical balance (Ohaus PR234M, Ohaus Corporation USA). Final yield measurement was performed in the second series of the experiment at thirteen WAS, coinciding with physiological indicators of harvest maturity.

Collection of soil samples

Soil samples were collected at 5 WAS from the potato rhizosphere at approximately 10-15 cm depth. For each pot, five soil cores were sampled using alcohol-sterilized spoons, with approximately a quarter spoon per core. The five subsamples were pooled and homogenized in sterile 50 mL Falcon tubes (Prasedya et al. 2022), placed in chilled boxes, and transferred to a −80°C freezer until further analysis.

DNA extraction, amplification, and sequencing of 16s rRNA library

Total soil DNA was extracted from 1 g of rhizosphere soil using the High Purity™ Soil DNA Isolation Kit (Canvas Biotech, Spain), following the manufacturer's recommended protocol. DNA concentration and purity were assessed spectrophotometrically using a NanoDrop 1000. Extracted DNA was stored at −20°C until library preparation.

Microbial diversity was analyzed based on the 16S rRNA gene, targeting the V3-V4 hypervariable region. Amplification of the V3-V4 region was performed as described by Prasedya et al. (2022), using Phusion High-Fidelity PCR Master Mix (New England Biolabs, MA, USA). Each reaction contained 2 µL of DNA template and the primers 341F (5′-CCTAYGGGRBGCASCAG-3′) and 806R (5′-GGACTACHVGGGTWTCTAAT-3′). The PCR conditions were as follows: initial denaturation at 98°C for 1 min; 30 cycles of denaturation at 98°C for 10 s, annealing at 50°C for 30 s, and extension at 72°C for 30 s; followed by a final extension at 72°C for 5 min.

Amplified products were mixed with 1× loading buffer containing SYBR Green and visualized on a 2% agarose gel. Bright bands of 400-450 bp were selected, pooled at equal density ratios, and purified using the Qiagen Gel Extraction Kit (Qiagen, Germany). Purified amplicons were sequenced using the Illumina iSeq 100 platform of next-generation sequencing (NGS) workflow, generating approximately ~114,000 and ~182,000 paired-end 2×150 bp reads per sample. Libraries were prepared using the NEBNext Ultra™ DNA Library Prep Kit for Illumina and quantified using Qubit fluorometry and qPCR. After merging, the average read length ranged from 406 to 418 bp.

Sequence analysis

Paired-end reads were first trimmed to remove barcode and primer sequences, and then merged using FLASH v1.2.7 to generate contigs. The resulting spliced sequences were designated as raw tags, which were subsequently quality-filtered using QIIME v1.7.0 (https://qiime.org/1.7.0/) to produce high-quality clean tags. These clean tags were compared against the SILVA reference database using the UCHIME algorithm to identify and remove chimeric sequences, resulting in a final set of effective tags.

Effective tags were clustered into operational taxonomic units (OTUs) using Uparse v7.0.1090, with sequences sharing ≥97% similarity grouped as the same OTU. Taxonomic classification of representative sequences was performed using the Mothur method against the SSU rRNA SILVA database via QIIME (http://www.arb-silva.de). Taxonomic ranks were assigned at a confidence threshold of 0.8-1.0, including levels from kingdom to species.

Statistical analysis

Differences in plant growth and yield were analyzed using analysis of variance (ANOVA), followed by post-hoc comparison using the least significant difference (LSD) test at a 0.05 significance level. Normality tests were performed based on the Anderson-Darling test, and one parameter (number of shots) that was not distributed normally was log-transformed before the ANOVA test. Statistical analysis was performed using Minitab for Windows 17.1. (https://minitab.informer.com/17.1/) and the graphs were made using GraphPad Prism version 10.0 for Windows (GraphPad Software, Boston, Massachusetts, USA, www.graphpad.com). Microbial alpha diversity metrics, including Shannon diversity, Simpson's index, Chao1, ACE, and phylogenetic diversity (PD), were calculated for the whole tree, were calculated to assess within-sample microbial richness and evenness. Beta diversity was evaluated using Bray-Curtis dissimilarity and visualized through principal coordinate analysis (PCoA), Venn diagrams, and weighted UniFrac-based phylogenetic trees. All plots were generated using GraphPad Prism software version 10.0 for Windows. Sequencing data were processed using QIIME v1.7.0 (https://qiime.org/1.7.0/), and the composition of the soil microbial community was visualized using Krona tools based on taxonomic profiles generated from QIIME outputs.

RESULTS AND DISCUSSION

Effect of different fertilization on growth and yield of potato plants

At five weeks after shoot emergence, the growth of potato plants was assessed to investigate the effects of different fertilization treatments. Different fertilization applications significantly influenced the growth of the potato plants. The significant effects were observed in the number of shoots, fresh weight, and dry weight but it did not alter the number of leaves and plant canopy diameter (Figure 1). The 50% inorganic fertilization in combination with biofertilization (CF50OF) resulted in the plant with a significantly higher number of shoots, plant fresh and dry biomass compared to the 50% inorganic fertilization treatment (CF50). Similarly, potato plants treated with 100% inorganic fertilization (CF 100) had a significantly higher number of shoots than the CF50 treatment, but no significant difference was observed for the number of leaves and canopy diameter. Interestingly, the growth of potato plants treated with 100% inorganic fertilizer (CF 100) was not significantly different from the 50% inorganic fertilization in combination with biofertilization treatment (CF50OF).

Reducing the inorganic fertilizer rate from 100% (CF100) to 50% (CF50), while maintaining equivalent levels of organic fertilizer in the growth media, significantly suppressed potato plant growth as evidenced by reductions in shoot number, fresh weight, and dry biomass. However, supplementing the lower inorganic fertilizer dose (CF50) with biofertilizer (CF50OF) restored plant growth to levels comparable with the full inorganic fertilizer treatment (CF100).

In this experiment, higher rates of inorganic fertilization enhanced above-ground potato growth, yet did not significantly affect tuber yield. Each plant produced between 380 and 420 g of tubers across all treatments, with a slight tendency toward higher yields in CF100 and CF50OF (Figures 1 and 2).

Impact of fertilization regimes on rhizosphere microbial diversity and abundance

Changes in alpha and beta diversity of the rhizosphere microbiome

In this study, the effect of different fertilization regimes on the richness and community structure of the soil microbiome in the potato rhizosphere was evaluated using alpha and beta diversity analysis. Variations in alpha diversity metrics, taxonomic overlap (Venn diagram), and beta diversity patterns are presented in Table 2 and Figure 3.

The Venn diagram (Figure 3.B) illustrated the distribution of 8,754 OTUs across the three fertilization treatments. Among these, 1,810 amplicon sequence variants were shared across all three fertilization treatments, though each treatment also harbored distinct sets of taxa. CF100 exhibited the highest number of treatment-specific OTUs (722), followed by CF50 and CF50OF with 430 and 336 unique taxa, respectively. Pairwise overlaps between treatments (313 for CF50-CF50OF, 259 for CF100-CF50OF,

and 345 for CF100-CF50) showed moderate levels of shared taxa, with the greatest overlap observed between CF100 and CF50.

The weighted Bray-Curtis heatmap (Figure 3.C), which visualized abundance-based dissimilarities, highlights shift in microbial community across different fertilization treatments. The greatest dissimilarity was observed between CF50 and CF100 ($\beta = 0.614 \pm 0.340$) followed by CF100 and CF50OF ($\beta = 0.571 \pm 0.396$), while the lowest dissimilarities occurred between CF50 and CF50OF ($\beta = 0.562 \pm 0.213$). The Bray-Curtis dissimilarity is an abundance-weighted metric reflecting both the presence and relative abundance of shared OTUs rather than the number of unique taxa. Although CF100 harbors the highest number of unique OTUs (722, compared to 430 in CF50 and 336 in CF50OF, Figure 3.B), many of these might be low-abundance taxa that contribute minimally to dissimilarity values, and therefore CF50 and CF50OF exhibit greater compositional similarity because they share a substantial proportion of high-abundance OTUs. Branch lengths in the phylogenetic tree (Figure 3.D) further illustrate genetic distances, with the scale bar representing 0.01 substitutions per site. Clustering patterns indicate treatment-specific shifts in microbial composition, with CF100 forming a distinct clade, suggesting greater divergence, shifts in microbial composition, with CF100 forming a distinct clade—suggesting greater divergence—while CF50 and CF50OF cluster more closely, indicating compositional similarity.

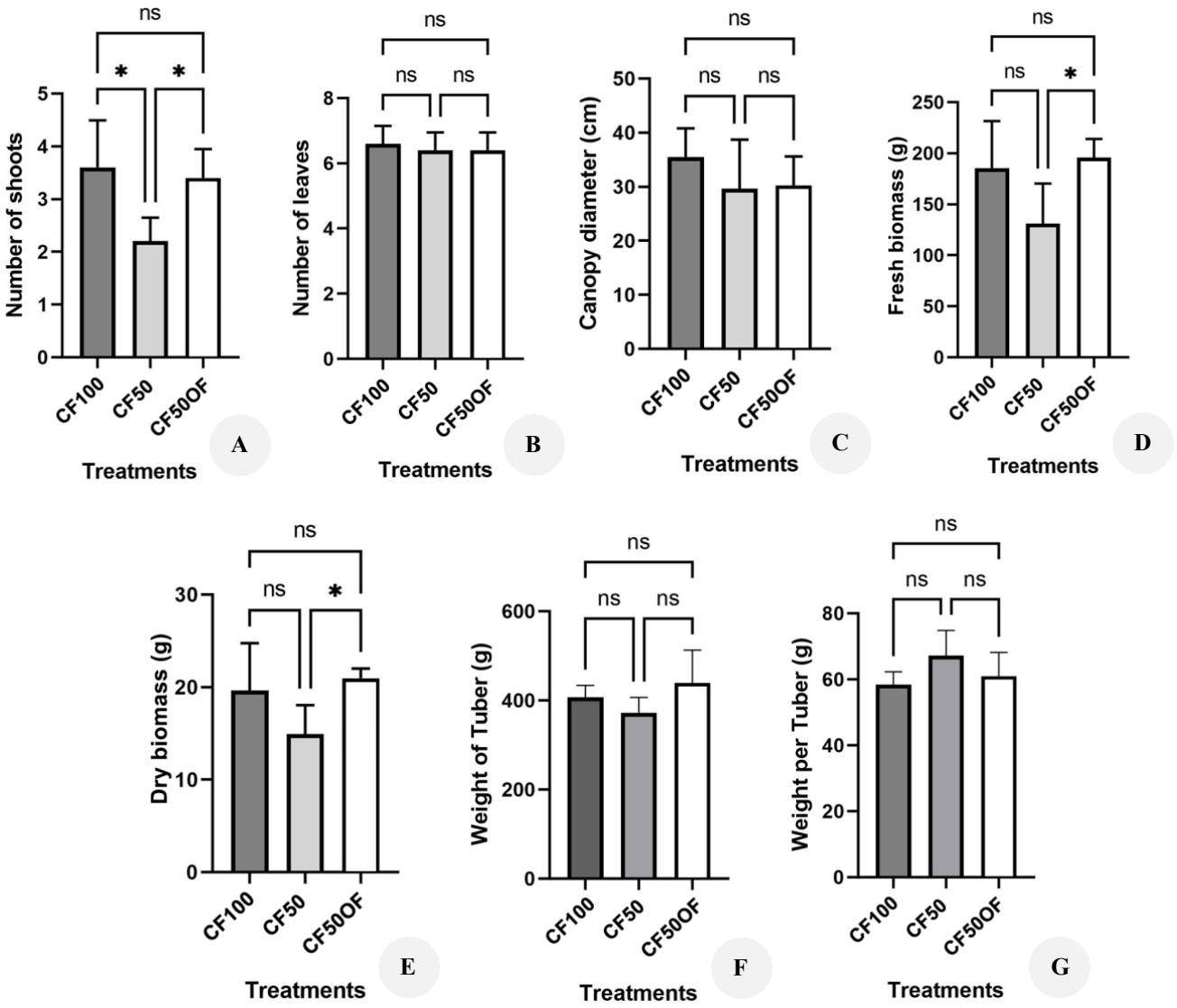

Figure 1. The effect of different fertilization treatments on growth of potato plants, i.e. A. the number of shoot, B. the number of leaves, C. the plant canopy diameter, D. plant fresh biomass, E. plant dry biomass, F. tuber weight per plant and G. weight of individual tuber; * denotes a significant different while ns indicates no significant different between treatments ($p < 0.05$). CF100: 100% recommended inorganic fertilization rate + organic fertilizer, CF50: 50% recommended inorganic fertilization rate + organic fertilizer, CF50OF: 50% recommended inorganic fertilization + organic fertilizer + biofertilization

Figure 2. Visualization of different growth of potato plants treated with: A-B. CF100, C-D. CF50, E-F. CF50OF

Changes in relative abundance of the rhizosphere microbiome

To gain deeper insight into how fertilization regimes shape the taxonomic structure of rhizosphere microbial communities, relative abundance profiling was undertaken. While diversity metrics revealed treatment-driven changes in richness, evenness, and community composition, the relative abundance data will provide further resolution by identifying which bacterial groups dominate under each fertilization strategy and how their proportional representation responds to nutrient input. The relative abundance profiles of rhizosphere microbiota at the phylum and genus levels under different fertilization treatments are illustrated in Figures 4 and 5.

In this experiment, the ten most abundant microbial phyla in all treatments, ranked from highest to lowest abundance, were: Proteobacteria, Firmicutes, Acidobacteria, Bacteroidata, Chloroflexi, Nitrospirota, Verrucomicrobiota Actinobacteriota, Myxococcota, and Gemmatimonadota, Plancomycota, (Figure 4.A). Across treatments, Firmicutes, Proteobacteria, Acidobacteria, and Bacteroidata dominated the microbial community, collectively accounting for 70 to 75% of the total abundance and exhibiting treatment-dependent shifts. A reduction in inorganic fertilizer dosage (CF50 and CF50OF treatments) increased the relative abundance of Proteobacteria by 40% (from 25 to 35%), while Firmicutes decreased by 50% (from 25 to 12.5%). Notably, Bacteroidota and Myxococcota nearly doubled in relative abundance under CF50OF compared to CF100 and CF50 treatments. These compositional differences were further illustrated in the z-score normalized enrichment heatmap (Figure 4.B), which revealed treatment-specific clustering and abundance gradients for the 35 most dominant phyla. Importantly, although Proteobacteria remained the most abundant phylum overall, it exhibited negative z-scores (blue shading) in the CF100 treatment, indicating lower-than-average relative abundance compared with its mean across treatments. In contrast, the light brown shading observed in CF50 and CF50OF reflects mild positive z-scores, signifying slightly higher-than-average enrichment. Shifts were also observed among the less abundant phyla, with Armatimonadota and Elusimicrobiota being enriched under reduced inorganic fertilizer treatments (CF50 and CF50OF). Collectively, these patterns highlight the strong influence of fertilization strategy on rhizosphere microbial community structure, affecting both dominant and rare taxa in abundance and enrichment profiles.

To further characterize treatment-specific microbial shifts, a heatmap was generated to visualize the relative abundance of rhizosphere bacterial taxa at the genus level across the three fertilization regimes (CF100, CF50, and CF50OF) (Figure 5). Distinct patterns of relative abundance and enrichment were also observed across fertilization treatments at the genus level. In this experiment, the ten most dominant genera, ranked from highest to lowest abundance, were *Enterococcus*, *Romboutsia*, *Lactobacillus*, *Ohtaekwangia*, *Pseudomonas, Candidatus_Udaeobacter, Escherichia_Shigella, Clostridium_sensu_stricto-1, Blrii4*, and *Streptococcus* (Figure 5.A). Amongst these, seven genera: *Blrii4*, *Lactobacillus*, *Ohtaekwangia*, *Romboutsia*, *Candidatus_Udaeobacter*, *Clostridium_sensu_stricto-1*, and *Pseudomonas* were identified as core genera. One genus, *Streptococcus*, was exclusively present in CF50 and CF50OF treatments, while *Enterococcus* was detected in CF50 and CF50OF regimes. Figure 5 also illustrates the relative abundance of these ten dominant genera across the three fertilization treatments. Specifically, *Lactobacillus* and *Romboutsia* were enriched under CF100 conditions. *Escherichia_Shigella, Candidatus_Udaeobacter*, and *Clostridium_sensu_stricto-1* were more abundant under CF50 treatment, while five genera, *Enterococcus*, *Ohtaekwangia*, *Pseudomonas*, *Sterptococcus*, and *Blrii4* were enriched under CF50OF conditions. Figure 5.B further confirmed that the CF50OF treatment enriched the highest number of genera (18), followed by the CF50 treatment (14 genera), whereas the CF100 treatment resulted in the lowest enrichment, with only 14 out of the 35 most abundant genera displaying positive z-scores. Across treatments, five genera were co-enriched under both CF100 and CF50, another five were shared between CF100 and CF50OF, and seven genera were jointly enriched under CF50 and CF50OF.

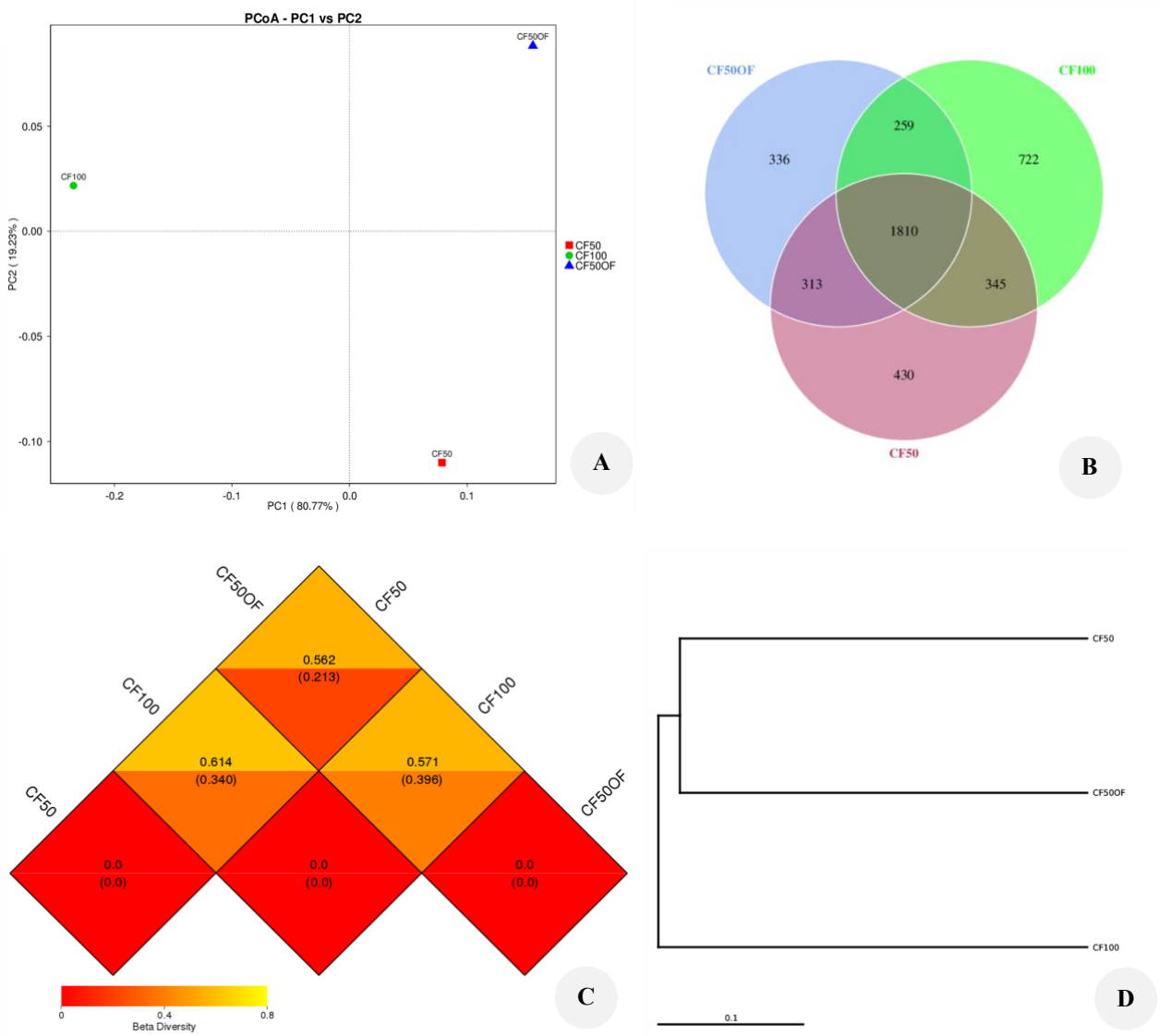

Figure 3. Multidimensional beta diversity and compositional analyses of rhizosphere microbial communities under differential fertilization regimes. A. Weighted Principal Coordinates Analysis (PCoA) based on Bray-Curtis dissimilarity, B. Venn diagram showing shared and unique OTUs among CF100, CF50, and CF50OF treatments, C. Heatmap of weighted Bray-Curtis dissimilarities between treatments emphasizes abundance-weighted community structure, and does not directly correlate with the number of unique OTUs, and D. Weighted UniFrac phylogenetic tree illustrating evolutionary relationships among microbial communities

Table 2. Alpha diversity indices (number of observed species, Shannon index, Simpson index, Chao1 index, ACE index, goods coverage, and PD whole tree) summarize the impact of different fertilization treatments on microbiome richness and phylogenetic diversity

Treatments	Observed-species	Shannon	Simpson	Chao1	ACE	Good-coverage	PD (wholetree)
CF100	3,136	9.616	0.995	3341.207	3364.708	0.992	287.370
CF50	2,898	9.480	0.994	3057.545	3066.055	0.993	286.222
CF50OF	2,718	9.271	0.993	3578.938	3077.685	0.989	172.841

Base on published literature, the bacterial genera were classified into six potential functional roles: (i) fermenters, gut microbiota, and organic matter degraders, (ii) nutrient (N, P, K) cyclers, (iii) plant growth hormone producers, (iv) biocontrol/bioremediators, (v) abiotic stress adapters, and (vi) other functions. Many genera contributed to multiple functional roles, consistent with the multifunctional nature of plant-associated and soil bacterial taxa reported in the literature.

Under CF100 treatment, 14 microbial genera were enriched, spanning 4 potential functional categories: fermenters, gut microbiota, and organic matter degraders

(8), nutrient cyclers (7), biocontrol/bioremediators (1), and other functions (3). In contrast, CF50 treatment enriched a broader potential functional diversity, enriched 14 genera distributed across 6 categories: fermenter, gut microbiota, and organic matter degraders (9), nutrient cycler (9), growth hormone producers (1), biocontroller/bioremediator (1), abiotic stress adapter (5), and other function (3). Notably, CF50OF treatment enriched the highest number of genera (18) within the 6 potential functional categories, including fermenters, gut microbiota organic matter degraders (8), organic matter degraders (10), nutrient cyclers (12), plant growth hormone producers (3), biocontrollers/ bioremediators (5), abiotic stress adapters (3) and other functions (4), with many genera contributing to multiple functional roles. These patterns suggest that reduced inorganic fertilization combined with organic inputs and biofertilizer (CF50OF) promotes a more functionally diverse and ecologically resilient rhizosphere microbiome.

Taken together, the microbiome analyses presented in this study confirm that fertilization strategy significantly influences microbial richness, community composition, functional potential, and phylogenetic diversity. Notably, the CF50OF treatment exhibited lower Shannon and Simpson diversity, but higher Chao1 index and a greater number of enriched genera with enriched functionally diverse microbial genera. These findings suggest that CF50OF promotes selective microbial enrichment rather than a broad expansion of overall diversity, a pattern that may contribute to improved potato growth.

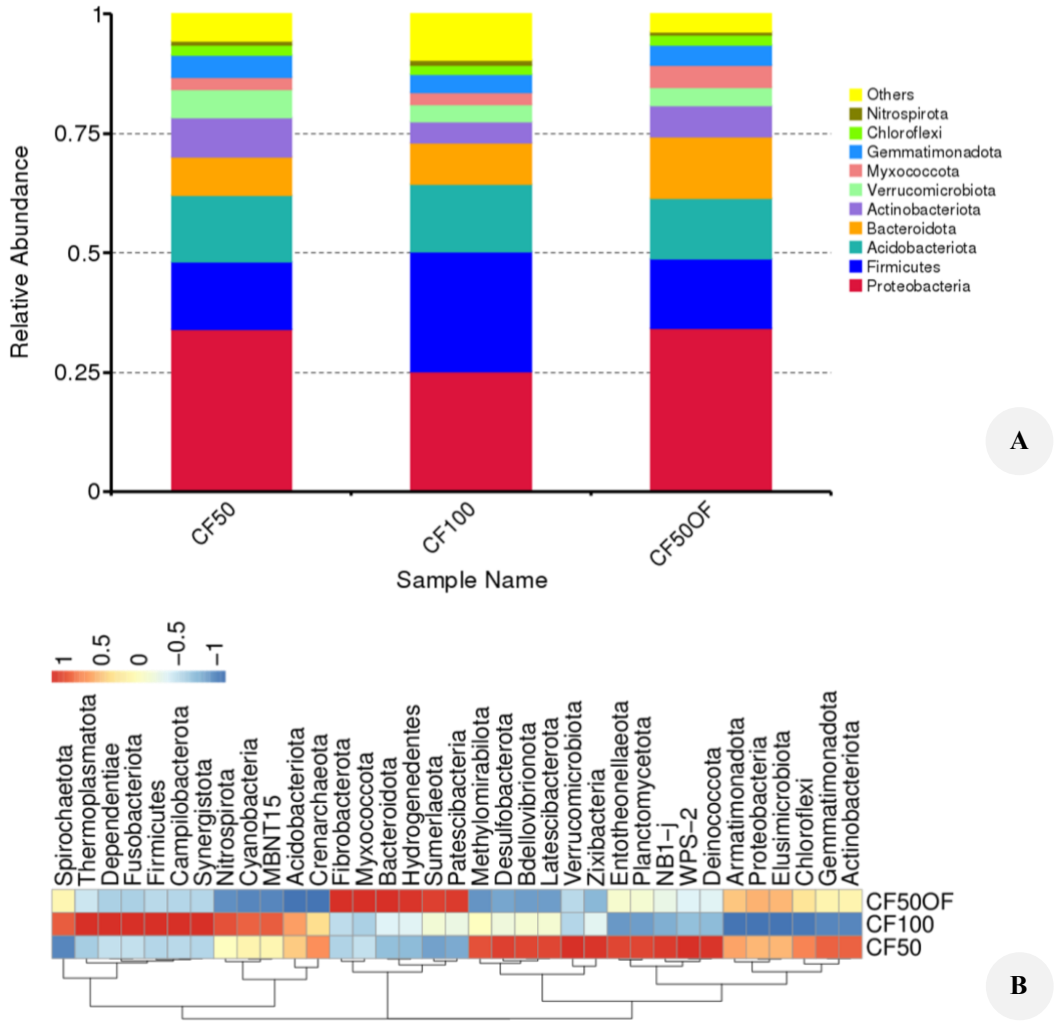

Figure 4. A. Illustration of the relative abundance of the ten most dominant bacterial phyla across treatments. Each bar represents the proportional composition of taxa, with color-coded segments corresponding to major phyla, including Proteobacteria, Firmicutes, Acidobacteriota, Bacteroidota, Actinobacteriota, Verrucomicrobiota, Myxococcota, Gemmatimonadota, Chloroflexi, and Nitrospirota. B. A heatmap showing z-score normalized differential enrichment of the 35 most dominant bacterial phyla across treatments. The color gradient reflects the enrichment scale, ranging from highest (+1, dark brown) to lowest (−1, dark blue), indicating relative shifts in microbial composition in response to treatment conditions

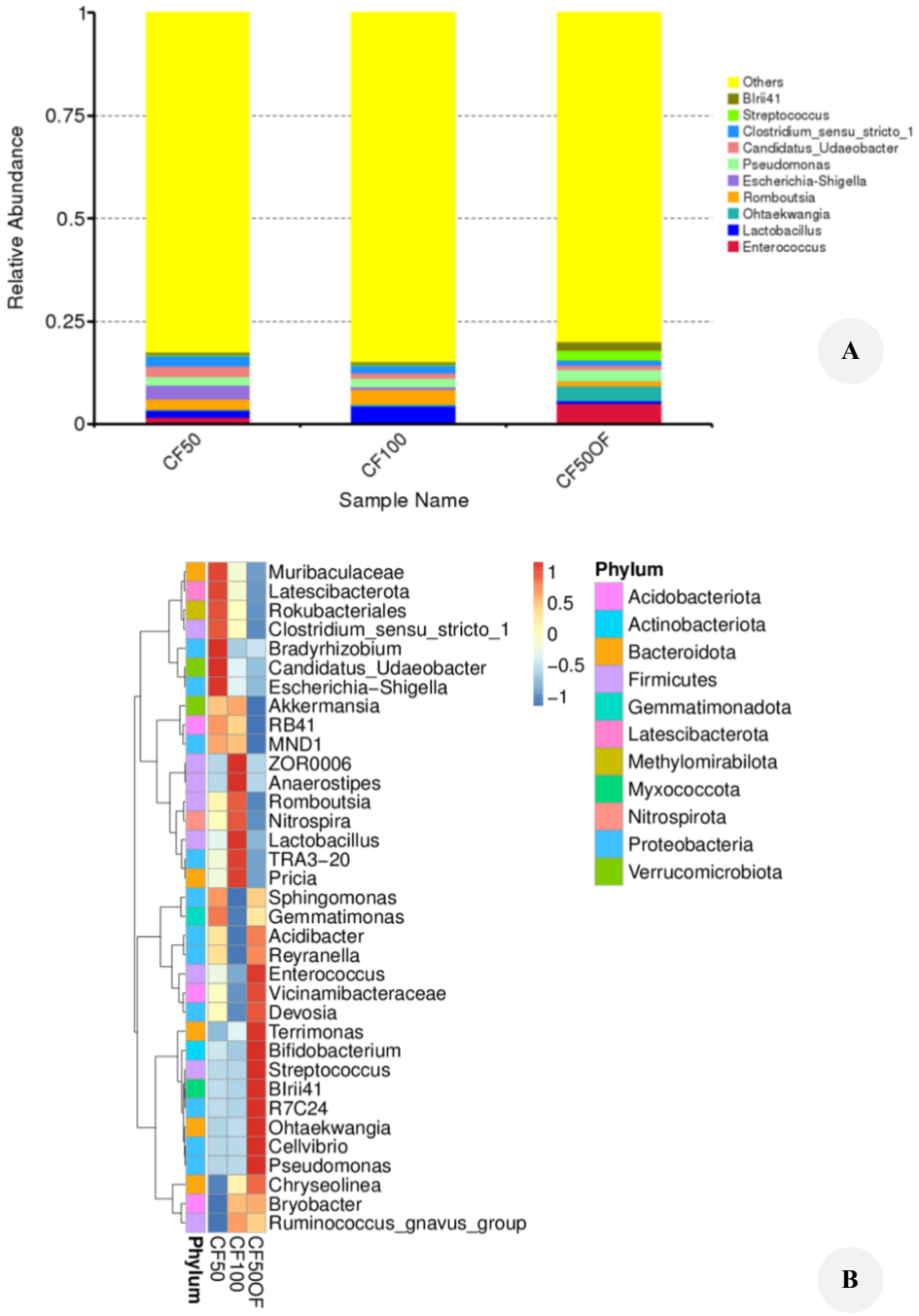

Figure 5. The relative abundance of the ten most dominant bacterial genera across treatments, expressed as proportions (0-1). A. Each bar represents the proportional composition of genera with color-coded segments corresponding to major genera, including *Enterococcus, Lactobacillus, Ohtaekwangia, Romboutsia, Escherichia-Shigella, Pseudomonas, Candidatus_Udaeobacter, Clostridium_sensu_stricto_1, Streptococcus,* and *Blrii4*, and a heatmap showing z-score normalized the differential enrichment of the 35 most dominant bacterial genera across treatments. B. The color gradient reflects the enrichment scale, ranging from highest (+1, dark brown) to lowest (−1, dark blue), indicating relative shifts in microbial composition in response to treatment conditions. Genera are hierarchically clustered based on abundance patterns, and each genus is color-coded by its corresponding phylum. Although the analysis included 35 genera spanning multiple phyla, only 11 phyla are represented in this figure; phyla not shown either contained low-abundance genera, were below detection thresholds, or were excluded during filtering for visualization clarity

Discussion

Potato growth performance was significantly influenced by fertilization strategy. Both CF100 (100% chemical + organic fertilizer) and integrated CF50OF (50% inorganic+ organic + biofertilizer) produced comparable vegetative growth; shoot number, leaf area, canopy size, and total biomass; all of which were higher than CF50 (50% chemical + organic fertilizer). Above-ground biomass traits,

including shoot number, leaf area, canopy size, and total biomass, are widely used as indicators of potato growth, as they directly influence photosynthetic capacity and subsequent tuber development (de Jesus Colwell et al. 2021; Neilson et al. 2021). Plant biomass reflects the accumulation of photosynthetically derived metabolites (Hu et al. 2021), which are strongly influenced by CO_2 concentration, nutrient availability, and water supply (Khan et al. 2022; Hu et al. 2025). Therefore, the higher biomass observed in CF100 and CF50OF treatments likely reflects enhanced nutrient availability compared to CF50, at which the inclusion of biofertilizer in CF50OF may have improved nutrient accessibility to levels comparable with CF100, thereby supporting greater metabolite accumulation and overall plant growth.

Despite notable differences in above-ground biomass, tuber yield did not differ significantly among treatments (Figure 1), indicating that increased potato vegetative growth and nutrient availability did not consistently translate into higher yield. Potato yield is primarily determined by the tuberization process, which encompasses stolon formation, tuber initiation, and tuber enlargement (Abeytilakarathna 2022; Singh et al. 2023). Stolon formation, originating from underground lateral buds, is influenced by the plant's vegetative status; thus, more vigorous above-ground growth may promote stolon development. In this study, plants treated with CF100 and CF50OF exhibited greater vegetative growth compared to CF50, and CF50OF also showed improved below-ground development (Figure 2, data not shown). Despite these growth differences, tuber yield remained statistically similar across treatments, likely due to suboptimal temperature conditions. Previous studies have demonstrated that tuberization, particularly the transition from stolon to tuber, is highly sensitive to environmental cues, especially temperature and photoperiod (Kondhare et al. 2021; Singh et al. 2023). The optimal temperature for tuber initiation is approximately 22°C, while tuber induction and maturation are best within a range of 14-25°C. Temperatures exceeding this range can inhibit tuber formation and growth (Singh et al. 2023). In Sembalun, where temperatures ranged from 18.6 to 29.2°C during the experiment, tuber initiation likely occurred, but subsequent development and maturation were constrained, limiting the impact of fertilization treatments on final yield.

Fertilization is a key agronomic management known to enhance plant growth by improving nutrient availability (Barlog et al. 2022; Al-Shammary et al. 2024). Along with using chemical fertilizer, in this study, chemical pesticide (Decis®) and fungicide (Zampro®) were applied weekly to all plants for pest and disease management. This practice reflects standard crop protection strategies commonly used by potato farmers in Sembalun. Although such inputs may influence rhizosphere microbial dynamics, their uniform application across all treatments minimized differential effects and allowed valid comparisons of fertilization and biofertilizer impacts. Under these conditions, we demonstrated that the combined application of biofertilizer with 50% inorganic fertilizer and organic fertilization (CF50OF) significantly enhanced plant growth compared to the use of 50% inorganic fertilizer and organic fertilization alone (CF50), and achieved growth levels comparable to those observed under 100% inorganic fertilization and organic fertilizer treatment (CF100). However, plant responses to fertilization are not solely governed by nutrient content in the soil; they are also mediated by complex interactions within the soil microbial community (Chen et al. 2024; Xing et al. 2025). To better understand the biological mechanism connecting fertilization strategies to plant performance and soil ecosystem dynamics, we conducted a comprehensive analysis of the potato rhizosphere microbiome under different fertilization regimes.

Our findings reveal that agronomic outcomes from different fertilization regimes closely align with shifts in the rhizosphere microbial community. Fertilization treatments significantly influenced both microbial richness and community composition associated with potato roots, as evidenced by variations in alpha and beta diversity metrics. In addition, relative abundance profiles at phylum and genus levels further highlight treatment-driven changes in microbial diversity and community structure, underscoring the role of fertilization in shaping soil microbial ecology.

Alpha diversity analysis (Table 2) showed that CF100 (100% inorganic + organic fertilization) supported the highest number of observed taxa and exhibited relatively even microbial distribution, indicative of a copiotrophic community structure. CF50 (50% inorganic + organic fertilization) demonstrated moderate richness and community complexity, while CF50OF (50% inorganic + organic + biofertilizer) showed fewer directly OTU but notably higher estimated richness (Chao1 index). This suggests the presence of rare or low-abundance taxa in CF50OF that may contribute disproportionately to functional diversity and ecological resilience (Zhou et al. 2022). These findings are in agreement with existing literature showing that inorganic fertilization often increases microbial abundance but can reduce diversity and functional redundancy, due to nutrient saturation and soil acidification. Excessive nutrient input, especially ammonium-based fertilization, triggers nutrient nitrification, releasing hydrogen ions and lowering soil pH (Zhang et al. 2017). This acidification can suppress specific microbial taxa and favor fast-growing copiotrophic taxa, leading to a homogenized community with reduced ecological buffering capacity (Li et al. 2024). Moreover, nutrient over-supply can disrupt microbial competition and niche partitioning, further narrowing community composition (Beltran-Gracia et al. 2021).

The beta diversity analyses, including weighted Bray-Curtis PCoA, abundance weighted heatmaps, and weighted UniFrac phylogenetic clustering, consistently showed that the integration of biofertilizer (CF50OF) influenced microbial community composition and structure (Figure 3). CF50OF samples appear to form distinct clusters and clades, indicating potential taxonomic and phylogenetic divergence from conventional treatments (CF50 and CF100). These findings are consistent with recent findings that biofertilizer application significantly alters microbial assemblages by introducing beneficial taxa and modifying root-microbe interaction (Kumar et al. 2023; Dzvene and Chiduza 2024).

Although no formal statistical testing (e.g., PERMANOVA or ANOSIM) was conducted, the observed

clustering patterns suggest that fertilization strategy may shape microbial assemblages. The Venn diagram (Figure 3.B) supports this, revealing a resilient core microbiome shared across all treatments, alongside treatment-specific enrichment. CF100 exhibited the highest number of unique OTUs (722), suggesting that full chemical fertilization may promote a more distinct microbial niche, often dominated by copiotrophic and fast-growing taxa (Wang et al. 2024). In contrast, CF50OF enriched a broader spectrum of rare and functionally diverse taxa, which are increasingly recognized for their contributions to ecosystem services such as nutrient cycling, organic matter decomposition, and stress tolerance (Chen et al. 2022; Gao et al. 2025).

These patterns underscore the influence of fertilization strategy on community assembly processes. Organic amendments, particularly biofertilizer, seem to promote taxonomic turnover and functional diversification, supporting a richer, more balanced, and compositionally distinct microbiome. This aligns with alpha diversity trends and OTU overlap patterns, which suggest that biofertilizer expands microbial niches and enhances ecological resilience. Across all treatments, the use of manure-based organic fertilizer provided a common baseline of carbon-rich inputs, improving soil structure, porosity, and microbial proliferation. Organic amendments are well documented to buffer soil pH, enhance nutrient retention, and foster microbial niche diversification (Guo et al. 2022; Pantelides et al. 2023; Chiodi et al. 2025). These foundational effects likely contributed to the shared core microbiome observed across CF100, CF50, and CF50OF, as evidenced by 1,810 OTUs common to all treatments (Figure 3). However, distinct microbial communities emerged depending on fertilization strategy.

The distinct clustering of CF100 in both Bray-Curtis dissimilarities and phylogenetic analyses observed (Figures 3.C and 3.D) further suggests that high chemical fertilization exerts a stronger selective pressure on microbial assemblages. In contrast, the closer clustering of CF50 and CF50OF indicates a more balanced microbial structure, likely supported by moderated nutrient availability and the presence of biofertilizer-derived microbial inoculants. These findings align with recent studies showing that fertilization regimes not only alter microbial richness and evenness but also restructure co-occurrence networks and functional guilds within the rhizosphere. For instance, Han et al. (2025) demonstrated that moderate organic fertilization (50-60% nitrogen replacement) optimized both microbial diversity and potato yield, with enriched taxa linked to nutrient cycling and plant growth promotion. Similarly, Chen et al. (2024) reported that excessive phosphorus fertilization disrupted microbial equilibrium and increased disease susceptibility, highlighting the importance of balanced inputs.

While diversity metrics and clustering analyses reveal how fertilization regimes shape microbial richness and community structure, they do not directly explain how these shifts influence nutrient availability and plant growth promotion. To better understand the functional implications of microbial compositional changes, we examined the relative abundance of key bacterial groups across treatments. This approach highlights not only which taxa dominate under specific nutrient regimes, but also how their prevalence may contribute to soil nutrient availability processes and plant-microbe interaction. By linking taxonomic enrichment to functional potential, we aim to gain deeper insight into the microbial mechanisms underpinning fertilization-driven changes in rhizosphere dynamics, links to plant growth and development.

At the phylum level, the microbial community was primarily composed of Proteobacteria, Firmicutes, Bacteroida and Acidobacteria, which collectively accounted for 70 to 75% of the total abundance. These phyla have consistently been reported as dominant across diverse soil and environmental conditions, such as farmland with different environments (Kim et al. 2021), sedimentary ecosystems (Zhang et al. 2020), saline-alkali environments (Dong et al. 2022), nutrient-enriched soils (Zhang et al. 2024), and under organic fertilizer application (Han et al. 2025). Their relative abundances are known to shift in response to environmental factors and fertilization strategies, reflecting their ecological adaptability and functional relevance.

In this experiment, a reduction in inorganic fertilizer dosage (CF50 and CF50OF treatments) increased the relative abundance of Proteobacteria by 40%, while Firmicutes declined by 50%. The addition of biofertilizer in CF50OF further enriched Bacteroidota and Myxococcota, nearly doubling their abundance compared to CF100 and CF50 treatments. These shifts reflect the ecological responsiveness of key bacterial phyla to fertilization strategies. Previous studies have shown that Acidobacteria and Proteobacteria communities are significantly influenced by soil pH, nutrient availability, and pesticide application (Kim et al. 2021). Similarly, Zhang et al. (2020) reported that Proteobacteria and Bacteroidota dominate sedimentary ecosystems, and Han et al. (2024) reported their response dynamically to organic inputs. Yu et al. (2024) highlighted the enrichment of Firmicutes and Myxococcota under lower nutrient supply, which increases decomposition of organic matter.

While phylum-level microbiome analysis provides a broad overview of microbial community structure, it often lacks the resolution necessary to uncover specific biological functions or detailed associations with plant-soil interactions. To address this limitation, we conducted microbiome functional enrichment at the genus level to better understand how different fertilization regimes influence the composition and functional potential of soil microbial communities. Genus-level abundance (Figure 5), and potential functional profiling inferred from the literature further confirmed that the CF50OF treatment supported a microbiome with greater potential functional enrichment. These microbial shifts are potentially associated with increased nutrient availability, plant hormone availability, a more complex microbial interaction network, and ultimately, improved plant growth performance. In the analysis, core microbial genera were identified across all treatments, such as *Lactobacillus*, *Romboutsia*, *Pseudomonas*, *Clostridium-sensu_stricto_1*, and *Acidibacter*, highlighting the presence of a resilient and functionally diverse rhizosphere microbiome under uniform organic fertilization. Despite all

treatments receiving the same amount of organic fertilizer, these genera remained consistently abundant even as inorganic fertilization dosages varied, suggesting their ecological stability and adaptability across varying inorganic input levels.

Fermentative genera such as *Lactobacillus* and *Romboutsia* contribute to organic matter turnover and microbial network stability (Liu et al. 2020; Chen et al. 2022; Tang et al. 2023) while *Pseudomonas* is widely recognized for its roles in nutrient mobilization, biocontrol, and plant growth promotion (Sah et al. 2021; Mehmood et al. 2023; Geng et al. 2024), *Clostridium_sensu_stricto_1* supports anaerobic decomposition and nitrogen transformation (Lian et al. 2025), and *Acidibacter* is often associated with carbon and nutrient cycling in acidic soils (Luo et al. 2023; Li et al. 2025). The persistence of these taxa across treatments suggests that organic inputs provide a stable ecological niche that supports core microbial functions, regardless of inorganic fertilizer dosage.

Under CF100 treatment (100% inorganic fertilizer plus organic input), a noticeably lower number of enriched microbial genera was observed. These genera were predominantly classified into four potential functional categories: fermenters, gut microbiota and organic matter degraders; nutrient cyclers; biocontroller/bioremediator, and other functions. This narrow functional profile suggests that high inorganic input may selectively favor fast-growing, copiotrophic taxa that thrive in nutrient-rich conditions but offer limited ecological breadth. While fermenters, gut microbiota, and organic matter degraders play essential roles in carbon turnover, the absence or reduced abundance of nutrient cyclers, hormone producers, and abiotic stress adapter taxa under CF100 indicates a constrained microbial ecosystem with lower functional redundancy. This narrow potential functional profile suggests that excessive organic fertilization may narrow the enrichment of the functional spectrum of the rhizosphere microbiome, reducing its capacity to buffer environmental fluctuation and support complex plant-microbe interactions. Such patterns are consistent with previous findings that excessive inorganic fertilization can reduce the abundance of beneficial taxa involved in plant-microbe interaction and signaling, disease suppression, and resilience to abiotic stress (Zhang et al. 2024; Han et al. 2025). As a result, the microbial community under CF100 may be less capable of sustaining long-term soil health and plant productivity, emphasizing the need for balanced fertilization strategies that preserve microbial functionality and ecological resilience.

Compared to CF100, the CF50 treatment (50% inorganic fertilizer plus organic input) fostered enrichment of a more functionally diverse microbial community, enriching more genera across six potential functional categories. This included a balanced representation of fermenters, gut microbiota, organic matter degraders, and nutrient cyclers, and one taxon potentially involved in plant growth promotion, one taxon potentially acts as biocontrol, five stress adaptation, and three taxa potentially acting as other functions. The broader functional spectrum observed under CF50 suggests that reducing inorganic input while maintaining organic fertilization creates a more favorable environment for diverse microbial niches, potentially enhancing soil multifunctionality and biological buffering capacity. However, the number of enriched genera within each functional category was lower than that observed under CF50OF. The CF50OF treatment, which combined reduced inorganic fertilizer with organic and biofertilizer inputs, enriched the highest number of genera (18) and exhibited the widest functional diversity, including fermenters, gut-associated microbiota and, organic matter degraders (13), nutrient cyclers (6), plant growth hormone producers (3), biocontrollers/bioremediators (5), abiotic stress adapters (1), and other functional groups (2). The elevated abundance of fermenters, organic matter degraders, and nutrient cyclers under CF50OF suggests enhanced nutrient turnover and bioavailability in the rhizosphere. Fermentative taxa contribute to the breakdown of complex organic substrates, releasing labile carbon and signaling compounds that support microbial interactions and root development (Byappanahalli et al. 2012; Liu et al. 2020; Murindangabo et al. 2023; Tang et al. 2023; Liang et al. 2024). Organic matter degraders accelerate decomposition processes, improving soil structure and nutrient release (Xiong et al. 2025), while nutrient cyclers facilitate key transformations such as nitrogen fixation, phosphorus solubilization, and sulfur metabolism (Yin et al. 2023; Geng et al. 2024; Sharma et al. 2025). Together, these functions create a biologically enriched soil environment conducive to plant growth. Moreover, the enrichment of three plant growth hormone producers, *Pseudomonas*, *Devosia*, and *Actinomyces*, and five biocontrol agents under CF50OF points to additional benefits beyond nutrient provisioning, such as improved root architecture, stress tolerance, and pathogen suppression. These microbial traits are known to enhance crop vigor and yield, especially under reduced chemical input (Sah et al. 2021; Chhetri et al. 2022; Xiao et al. 2022; Geng et al. 2024). The observed microbial enrichment under CF50OF aligns with previous studies demonstrating that integrated fertilization strategies promote beneficial microbial communities linked to improved plant productivity and soil health (Han et al. 2025; Ng et al. 2025). Overall, CF50OF fosters microbial recruitment, functional specialization, and ecological resilience, resulting in improved nutrient use efficiency and plant performance comparable to that observed under full fertilization (CF100) while offering both agronomic and ecological advantages. By supporting a diverse and functionally integrated microbial community, CF50OF represents a promising approach for biologically enriched and sustainable agroecosystems. This strategy not only supports crop productivity but also enhances soil health, microbial stability, and long-term nutrient cycling capacity, key pillars for climate-smart agriculture and SDG-aligned farming systems. However, the current study does not employ functional inference tools such as PICRUSt2, Tax4Fun, or HUMAnN, nor does it utilize metagenomic or transcriptomic data. Therefore, the functional narratives presented (e.g., nutrient cycling, hormone production, biocontrol) are based on genus-level taxonomic profiles and known ecological roles from published literature, rather than direct functional validation. The plant-microbiome

relationships described here are inferred potential functional roles from published literature but not validated experimentally. and should be interpreted with caution. Future research should incorporate functional inference and metagenomic validation to rigorously validate these associations and establish mechanistic links between microbial community dynamics and plant performance under CF50OF.

The CF50OF treatment incorporated a biofertilizer containing *Azospirillum* sp., *P. fluorescens*, and *T. asperellum.* However, only *Pseudomonas* and select indigenous taxa were significantly enriched in the rhizosphere. *Pseudomonas* spp. is known for its rapid colonization, metabolic versatility, and strong interactions with native soil microbiota, often leading to enhanced abundance and activity in rhizosphere environments (Sah et al. 2021; Geng et al. 2024; Mehmood et al. 2025). In contrast, *Azospirillum* was not detected, possibly due to competitive exclusion, suboptimal environmental conditions, or host plant selectivity; factors known to influence its variable colonization in potato systems (Kargapolova et al. 2020; Naqqash et al. 2022; Nievas et al. 2023). Additionally, strain-specific traits and inoculant viability may have affected its establishment. It is also possible that primer bias in the 16S rRNA sequencing protocol contributed to its non-detection, as universal primers may vary in their ability to amplify specific taxa. Future studies should consider taxon-specific primers or complementary molecular approaches to improve detection sensitivity (Na et al. 2023; Sunthornthummas et al. 2025). Meanwhile, *T. asperellum* was not observed in the microbiome dataset due to methodological constraints. As a fungus, *Trichoderma* cannot be detected using 16S rRNA gene sequencing, which targets bacterial and archaeal taxa. Fungal profiling requires ITS region sequencing, which was not employed in this study (Wagg et al. 2019; Jiao et al. 2021; Song et al. 2024). Therefore, while *Trichoderma* may have contributed to plant growth or pathogen suppression, its presence could not be confirmed through the bacterial-focused analysis. Accordingly, future studies should incorporate ITS-based fungal profiling to enable a more complete assessment of biofertilizer effects and microbial community dynamics.

Overall, these results reinforce the value of integrated fertilization strategies that combine inorganic, organic, and biofertilizer inputs to sustain potato crop growth while enhancing microbial functionality and ecological resilience. The CF50OF treatment, despite using only half the chemical fertilizer, matched CF100 in potato biomass, demonstrating that biofertilizer-driven microbial synergy can compensate for lower synthetic nutrient levels. This has important implications that continuous application of organic and biofertilizers should be encouraged, particularly in systems aiming to reduce environmental impact and improve soil health. Although chemical analyses of the manure and topsoil were conducted before planting, temporal nutrient profiling in both soil and plant tissues was not performed during the experiment. This limits our ability to directly link fertilization inputs with nutrient availability, plant uptake, and microbiome responses. Future studies should incorporate sequential nutrient measurements to elucidate these relationships better. In addition to primer bias and fungal detection constraints, we acknowledge that the absence of extraction blanks, no-template PCR controls, and mock communities limits our ability to detect and quantify potential contamination. While sterile protocols were followed, future studies should incorporate these controls to strengthen data reliability and interpretive confidence. The future research should focus on optimizing biofertilizer formulations, understanding long-term microbial dynamics, and developing locally adapted fertilization models that align with climate-smart agriculture and Sustainable Development Goals.

In conclusion, this study demonstrates that integrating biofertilizers with reduced inorganic inputs while maintaining organic inputs (CF50OF) can sustain potato growth while enhancing rhizosphere microbial functionality and soil health. Although CF50OF exhibited lower Shannon and Simpson diversity indices and fewer observed taxa compared to CF100, it showed higher Chao1 richness and more diverse functional enrichment. This suggests that CF50OF supports a specialized microbial community with greater functional potential, likely driven by biofertilizer-mediated recruitment of fermentative, carbon-degrading, nutrient-recycling, plant-growth-promoting, and stress-tolerant taxa. These taxa contribute to nutrient cycling, microbial synergy, and improved nutrient use efficiency, compensating for reduced chemical inputs. The comparable growth achieved by CF50OF and CF100 underscores the catalytic role of biofertilizer in sustaining growth through functional microbial enhancement rather than taxonomic diversity alone. These findings highlight the potential of integrated fertilization strategies to reduce chemical dependency without compromising growth. However, these conclusions are limited by the use of 16S amplicon sequencing alone, which excludes fungal taxa and may underrepresent certain bacterial groups; the absence of PERMANOVA for beta-diversity validation; and the reliance on inferred functional roles rather than metagenomic confirmation. Future studies should incorporate ITS sequencing, functional prediction tools, metagenomic or transcriptomic validation, contamination controls, and nutrient profiling over time. Field-scale trials are also needed to assess long-term stability, fertilizer-use efficiency, and practical suitability of CF50OF for climate-smart and sustainable potato production, and Sustainable Development Goals will be essential.

ACKNOWLEDGEMENTS

This research was funded by the Universitas Mataram, Indonesia. The authors gratefully acknowledge this support, which contributed to the advancement of scholarly work in sustainable development.

REFERENCES

Abeytilakarathna PD. 2022. Factors affecting stolon formation and tuberization in potato: A review. Agric Rev 43 (1): 91-97. https://doi.org/10.18805/ag.R-187.

Al-Shammary AAG, Al-Shihmani LSS, Fernández-Gálvez J, Caballero-Calvo A. 2024. Optimizing sustainable agriculture: a comprehensive review of agronomic practices and their impacts on soil attributes. J Environ Manag 364: 121487. https://doi.org/10.1016/j.jenvman.2024.121487.

Barłóg P, Grzebisz W, Łukowiak R. 2022. Fertilizers and fertilization strategies mitigating soil factors constraining efficiency of nitrogen in plant production. Plants 11 (14): 1855. https://doi.org/10.3390/plants11141855

Beltrán-García MJ, Martínez-Rodríguez A, Olmos-Arriaga I, Valdés-Salas B, Mascio PD, White JF. 2021. Nitrogen fertilization and stress factors drive shifts in microbial diversity in soils and plants. Symbiosis 84: 379-390. https://doi.org/10.1007/s13199-021-00787-z.

Betancur CB, Lang B, Russell DJ. 2023. Organic nitrogen fertilization benefits selected soil fauna in global agroecosystems. Biol Fertil Soils 59: 1-162. https://doi.org/10.1007/s00374-022-01677-2.

BPS [Badan Pusat Statistik]. 2025. Produksi tanaman sayuran. https://www.bps.go.id/id/statistics-table/2/NjEjMg==/production-of-vegetables.html. [Indonesian]

Buckseth T, Kuma, V, Sharma AK, Sood S, Dalamu, Bhardwaj V, Sadawarti MJ, Challam C, Mangal V, Singh B. 2024. An overview of seed potato production: National and International perspectives. In: Buckseth T, Kumar V, Sharma AK (eds). Approaches for Potato Crop Improvement and Stress Management. Springer. https://doi.org/10.1007/978-981-97-1223-6_17.

Byappanahalli MN, Nevers MB, Korajkic A, Staley ZR, Harwood VJ. 2012. Enterococci in the environment. Microbiol Mol Biol Rev 76 (4): 685-706. https://doi.org/10.1128/MMBR.00023-12.

Chabani H, Tarchoun N, Amami R, Saadaoui W, Mezghani N, Alexopoulos AA, Petropoulos SA. 2025. Investigating the effects of optimized mineral fertilization on plant growth, physiological traits, tuber yield, and biochemical contents of the potato crop. Horticulturae 11 (1): 11. https://doi.org/10.3390/horticulturae11010011.

Chea L, Alhussein M, Karlovsky P, Pawelzik F, Naumann M. 2024. Adaptation of potato cultivars to phosphorus variability and enhancement of phosphorus efficiency by *Bacillus subtilis*. BMC Plant Biol 24: 1176. https://doi.org/10.1186/s12870-024-05868-x.

Chen Q, Song Y, An Y, Lu Y, Zhong G. 2024. Soil microorganisms: Their role in enhancing crop nutrition and health. Diversity 16 (12): 734. https://doi.org/10.3390/d16120734.

Chen Y, Li Q, Wu W, Liu X, Cheng J, Deng X, Cai X, Yuan W, Xie J, Zhang S, Wang B. 2022. Effects of lightning on rhizosphere soil properties, bacterial communities, and active components of *Camellia sinensis* var. *assamica*. Front Microbiol 13: 911226. https://doi.org/10.3389/fmicb.2022.911226.

Chhetri G, Kim I, Kang M, Kim J, So Y, Seo T.2022. *Devosia rhizoryzae* sp. nov., and *Devosia oryziradicis* sp. nov., novel plant growth-promoting members of the genus *Devosia*, isolated from the rhizosphere of rice plants. J Microbiol 60: 1-10. https://doi.org/10.1007/s12275-022-1474-8.

Chiodi C, Zardinoni G, Stevanato P, Giagnoni L, Carletti P, Oustrière N, Sæbø A, Persson T, Szulc W, Rutkowska B, Mench M, Renella G. 2025. Organic amendments influence soil properties, microbial diversity, and winter barley traits in a five-year field trial. Chem Biol Technol Agric 12: 87. https://doi.org/10.1186/s40538-025-00810-1.

de Jesus Colwell F, Souter J, Bryan GJ, Compton LJ, Boonham N, Prashar A. 2021. Development and validation of methodology for estimating potato canopy structure for field crop phenotyping and improved breeding. Front Plant Sci 12: 612843. https://doi.org/10.3389/fpls.2021.612843.

Dong M, Hu S, Lv S, Rong F, Wang X, Gao X, Xu Z, Xu Y, Liu K, Liu A. 2022. Recovery of microbial community in strongly alkaline bauxite residues after amending biomass residue. Ecotoxicol Environ Saf 232: 113281. https://doi.org/10.1016/j.ecoenv.2022.113281.

Dzvene AR, Chiduza C. 2024. Application of biofertilizers for enhancing beneficial microbiomes in push-pull cropping systems: A review. Bacteria 3: 271-286. https://doi.org/10.3390/bacteria3040018.

Fang X, Xiang Z, Ma H, Wang F, Wang Q, Li P, Zheng S. 2023. Effect of N fertilizer dosage and base/topdressing ratio on potato growth characteristics and yield. Agronomy 13 (3): 909. https://doi.org/10.3390/agronomy13030909.

FAO [Food and Agriculture Organization]. 2023. FAOSTAT. Food and Agriculture Organization of the United Nations. Retrieved from https://www.fao.org/faostat/en.

Gao W, Chen S, Yu X, Chen S, Wan C, Wang Y, Wu P, Li Q. 2025. Three local plants adapt to the ecological restoration of abandoned lead-zinc mines through the assembly of rhizosphere bacterial communities. Front Microbiol 16: 1533965. https://doi.org/10.3389/fmicb.2025.1533965.

Geng Y, Ding Y, Zhou P, Wang P, Peng C, Li D. 2024. Soil microbe-mediated carbon and nitrogen cycling during primary succession of biological soil crusts in tailings ponds. Sci Total Environ 894: 164969. https://doi.org/10.1016/j.scitotenv.2023.164969.

Gunadi N, Pronk A. 2023. Identifying key factors to improve productivity and reduce the environmental impact of potato farms in West Java, Indonesia. E3S Web Conf 373: 04019. https://doi.org/10.1051/e3sconf/202337304019.

Guo L, Nie Z, Zhou J, Zhang S, An F, Zhang L, Tóth T, Yang F, Wang Z. 2022. Effects of different organic amendments on soil improvement, bacterial composition, and functional diversity in saline-sodic soil. Agronomy 12 (10): 2294. https://doi.org/10.3390/agronomy12102294.

Han X, Yang J, Li Q, Zhang L, Li Y, Gai Y, Sang Y and Zhang Z. 2025. Organic fertilizer application rates affect rhizosphere microbial communities and yield optimization in potato (*Solanum tuberosum* L. V7). Front Microbiol 16: 1651178. https://doi.org/10.3389/fmicb.2025.1651178.

Hu HJ, Xu K, He LC. Wang GX. 2021. A model for the relationship between plant biomass and photosynthetic rate based on nutrient effects. Ecosphere 12 (8): e03678. https://doi.org/10.1002./ecs2.3678.

Hu M, Chen HY, Chang SX, Leuzinger S, Dukes JS, Langley JA, Bader MF, VanSundert K, Liao H, Ma Z. 2025. Plant functional traits affect biomass responses to global change: A meta-analysis. J Ecol 113: 2046-2065. https://doi.org/10.1111/1365-2745.70076.

Jennings SA, Koehler AK, Nicklin KJ, Deva C, Sait SM, Challinor AJ. 2020. Global potato yields increase under climate change with adaptation and CO_2 fertilisation. Front Sustain Food Syst 4: 519324. https://doi.org/10.3389/fsufs.2020.519324.

Ji L, Ni K, Wu Z, Zhang J, Yi X, Yang X, Ling N, You Z, Guo S, Ruan J. 2020a. Effect of organic substitution rates on soil quality and fungal community composition in a tea plantation with long-term fertilization. Biol Fertil Soils 56: 633-646. https://doi.org/10.1007/s00374-020-01439-y.

Ji Y, Conrad R, Xu H. 2020b. Responses of archaeal, bacterial, and functional microbial communities to growth season and nitrogen fertilization in rice fields. Biol Fertil Soils 56: 81-95

Jiao S, Peng Z, Qi J, Gao J, Wei G. 2021. Linking bacterial-fungal relationships to microbial diversity and soil nutrient cycling. mSystems 6 (2): e01052-20. https://doi.org/10.1128/mSystems.01052-20.

Kargapolova KY, Burygin GL, Tkachenko OV, Evseeva NV, Belimov AA. 2020. Effectiveness of inoculation of in vitro-grown potato microplants with *Azospirillum* spp. Plant Cell Tissue Organ Cult 141: 351-359. https://doi.org/10.1007/s11240-020-01791-9.

Khan A, Yan L, Hasan MD, Wang W, Xu K, Zou G, Liu XD, Fang XW. 2022. Leaf traits and leaf nitrogen shift photosynthesis adaptive strategies among functional groups and diverse biomes. Ecol Indic 141: 109098. https://doi.org/10.1016/j.ecolind.2022.109098.

Kim HS, Lee SH, Jo HY, Finneran KT, Kwon MJ. 2021. Diversity and composition of soil *Acidobacteria* and *Proteobacteria* communities as a bacterial indicator of past land-use change from forest to farmland. Sci Total Environ 797: 148944. https://doi.org/10.1016/j.scitotenv.2021.148944.

Kirchgesser J, Hazarika M, Bachmann-Pfabe S, Dehmer KJ, Kavka M, Uptmoor R. 2023. Phenotypic variation of root-system architecture under high P and low P conditions in potato (*Solanum tuberosum* L.). BMC Plant Biol 23: 68. https://doi.org/10.1186/s12870-023-04070-9.

Kondhare KR, Kumar A, Patil NS, Malankar NM, Saha K, Banerjee AK. 2021. Development of aerial and below-ground tubers in potato is governed by photoperiod and epigenetic mechanisms. Plant Physiol 187 (3): 1071-1086. https://doi.org/10.1093/plphys/kiab409.

Kumar M, Ansari WA, Zeyad MT, Singh A, Chakdar H, Kumar A, Farooqi MS, Sharma A, Srivastava S, Srivastava AK. 2023. Core microbiota of wheat rhizosphere under Upper Indo-Gangetic plains and their response to soil physicochemical properties. Front Plant Sci 14:1186162. https://doi.org/10.3389/fpls.2023.1186162.

Li S, Tang S, Ju X, Zhu Z, Zhang Y, Chen H, Jin K. 2024. Soil acidification drives the negative effects of nitrogen enrichment on soil microbial biomass at the global scale. Plant Soil 503: 517-528. https://doi.org/10.1007/s11104-024-06600-2.

Li Y, Zhang X, Chen H. 2025. The invisible architects: Microbial communities and their transformative role in soil health. Environ Microbiome 20: 45-58. https://doi.org/10.1186/s40793-025-00694-6.

Lian T, Yin F, Cao Q, Zhou T, Zhang F, Sun X, Cai Y, Dong H. 2025. Enhancing lactic acid production by organic loading rate regulation during anaerobic co-fermentation: Insights into metabolic and bacterial responses. Environ Technol Innov 40: 104525. https://doi.org/10.1016/j.eti.2025.104525.

Liang Y, Wang Z, Gao N, Qi X, Zeng J, Cui K, Lu W, Bai S. 2024. Variations and interseasonal changes in the gut microbial communities of seven wild fish species in a natural lake with limited water exchange during the closed fishing season. Microorganisms 12 (4): 800. https://doi.org/10.3390/microorganisms12040800.

Liu H, Li S, Qiang R, Lu E, Li C, Zhang J, Gao Q. 2022. Response of soil microbial community structure to phosphate fertilizer reduction and combinations of microbial fertilizers. Front Environ Sci 10: 899727. https://doi.org/10.3389/fenvs.2022.899727.

Liu Q, Zong C, Dong Z, X, Zhu J, Li J, Zhang J, Saho T. 2020. Effects of cellulolytic lactic acid bacteria on the lignocellulose degradation, sugar profile, and lactic acid fermentation of high-moisture alfalfa ensiled in low-temperature seasons. Cellulose 27: 7955-7965. https://doi.org/10.1007/s10570-020-03350-z.

Lombardo S, Pandino G, Mauromicale G. 2020. Optimizing nitrogen fertilization to improve qualitative performances and physiological and yield responses of potato (*Solanum tuberosum* L.). Agronomy 10 (3): 352. https://doi.org/10.3390/agronomy10030352.

Luo J, Banerjee S, Ma Q, Liao G, Hu B, Zhao H, Li T. 2023. Organic fertilization drives shifts in microbiome complexity, and keystone taxa increase the resistance of microbial-mediated functions to biodiversity loss. Biol Fertil Soils 59: 441-458 https://doi.org/10.1007/s00374-023-01719-3.

Makani M, Zotarelli L, Sargent S, Huber D, Sims C. 2020. Nitrogen fertilizer rate affects yield and tuber quality of drip-irrigated tablestock potatoes (*Solanum tuberosum* L.) grown under subtropical conditions. Am J Potato Res 97: 605-614.

Mehmood N, Saeed M, Zafarullah S, Hyder S, Rizvi ZF, Gondal AS, Jamil N, Iqbal R, Ali B, Ercisli S, Kupe M. 2023. Multifaceted impacts of plant-beneficial *Pseudomonas* spp. in managing various plant diseases and crop yield improvement. ACS Omega 8 (25): 22296-22315. https://doi.org/10.1021/acsomega.3c00870.

Murindangabo YT, Kopecký M, Perná K, Nguyen TG, Konvalina P, Kavková M. 2023. Prominent use of lactic acid bacteria in soil-plant systems. Appl Soil Ecol 189: 104955. https://doi.org/10.1016/j.apsoil.2023.104955.

Na HS, Song Y, Yu Y, Chung J. 2023. Comparative analysis of primers used for 16S rRNA gene sequencing in oral microbiome studies. Methods Protoc 6 (4): 71. https://doi.org/10.3390/mps6040071.

Naqqash T, Malik KA, Imran A, Hameed S, Shahid M, Hanif MK, Majeed A, Iqbal MJ, Qaisrani MM, van Elsas JD. 2022. Inoculation with *Azospirillum* spp. acts as the liming source for improving the growth and nitrogen use efficiency of potato. Front Plant Sci 13: 929114. https://doi.org/10.3389/fpls.2022.929114.

Neilson JAD, Smith AM, Mesina L, Vivian R, Smienk S, Koyer DeD. 2021. Potato tuber shape phenotyping using RGB imaging. Agronomy 11: 1781. https://doi.org/10.3390/agronomy11091781.

Ng FL, Li TC, Wang E, Lee TY, Chen GT, Su JF, Chen WL. 2025. *Bacillus*-based biofertilizer influences soil microbiome to enhance soil health for sustainable agriculture. Sustainability 17: 6293. https://doi.org/10.3390/su17146293.

Nievas S, Coniglio A, Takahashi WY, López GA, Larama G. 2023. Unraveling *Azospirillum*'s colonization ability through microbiological and molecular evidence. J Appl Microb 134 (4): lxad071. https://doi.org/10.1093/jambio/lxad071.

Nurhidayah N, Nikmatullah A, Haryanto H. 2023. Efektivitas pupuk hayati bactoplus dalam meningkatkan efisiensi pemupukan npk pada tanaman kentang (*Solanum tuberosum* L.) varietas Chitra. Jurnal Sains Teknologi Lingkungan 9 (3): 391-400. https://doi.org/10.29303/jstl.v9i3.472.

Pantelides IS, Stringlis IA, Finkel OM, Mercado-Blanco J. 2023. Organic amendments-microbial communities and their role in plant fitness and disease suppression. Front Plant Sci 14: 1213092. https://doi.org/10.3389/fpls.2023.1213092.

Prasedya ES, Kurniawan NSH, Kirana IAP, Ardiana N, Abidin AS, Ilhami BTK, Jupri A, Widyastuti, Sunarpi H, Nikmatullah A. 2022. Seaweed fertilizer prepared by em-fermentation increases the abundance of beneficial soil microbiome in paddy (*Oryza sativa* L.) during the vegetative stage. Fermentation 8 (2): 46. https://doi.org/10.3390/fermentation8020046.

Pronk AA, Gunadi N, Hermelink MI, Hengsdijk H, Jindo K, Silva JV. 2025. Opportunities to narrow potato yield gaps and increase resource use efficiency in West Java, Indonesia. Potato Res 68: 1137-1158. https://doi.org/10.1007/s11540-024-09778-1.

Raman J, Kim JS, Choi KR, Eun H, Yang D, Ko YJ, Kim SJ. 2022. Application of lactic acid bacteria (LAB) in sustainable agriculture: Advantages and limitations. Intl J Mol Sci 23: 7784. https://doi.org/10.3390/ijms23147784.

Ran T, Li J, Liao K, Zhao Y, Yang G, Long J. 2023. Effects of biochar amendment on bacterial communities and their function predictions in a microplastic-contaminated *Capsicum annuum* L. Soil Environ Technol Innov 31: 103174. https://doi.org/10.1016/j.eti.2023.103174.

Ren J, Shen YC, Shen FP. 2025. Optimizing fertilization strategies for high-yield potato crops. Mol Soil Biol 16 (1): 1-15. https://doi.org/10.5376/msb.2025.16.0001.

Sah S, Krishnani S, Singh R. 2021. Pseudomonas mediated nutritional and growth promotional activities for sustainable food security. Curr Res Microb Sci 2: 100084. https://doi.org/10.1016/j.crmicr.2021.100084.

Sharma R, Kumar D, Kapoor N, Ohri P. 2025. Insights into the biodiversity, mechanisms, and plant growth-promoting effects of *Bradyrhizobium* and their potential in sustainable agriculture. Pedosphere 2025. https://doi.org/10.1016/j.pedsph.2025.06.017.

Singh P, Arif Y, Siddiqu H, Upadhyaya CP, Pichtel J, Haya S. 2023. Critical factors responsible for potato tuberization. Bot Rev 89: 421-437. https://doi.org/10.1007/s12229-023-09289-7.

Song B, Wang T, Wan C, Cai Y, Mao L, Ge Z, Yang N. 2024. Diversity patterns and drivers of soil bacterial and fungal communities in a muddy coastal wetland of China. J Fungi 10 (11): 770. https://doi.org/10.3390/jof10110770.

Sunthornthummas S, Wasitthankasem R, Phokhaphan P, Sudtachat N, Wilantho A, Ngamphiw C, Chareanchim W, and Tongsima S. 2025. Unveiling the impact of 16S rRNA gene intergenomic variation on primer design and gut microbiome profiling. Front Microbiol 16: 1573920. https://doi.org/10.3389/fmicb.2025.1573920.

Tang J, Su L, Fang Y, Wang C, Meng L, Wang J, Zhang J, Xu W. 2023. Moderate nitrogen reduction increases nitrogen use efficiency and positively affects microbial communities in agricultural soils. Agriculture 13 (4): 796. https://doi.org/10.3390/agriculture13040796.

Tiwari JK, Buckseth T, Singh RK, Kumar M, Kant S. 2020. Prospects of improving nitrogen use efficiency in potato: Lessons from transgenics to genome editing strategies in plants. Front Plant Sci 11: 597481. https://doi.org/10.3389/fpls.2020.597481.

Wagg C, Schlaeppi K, Banerjee S, Kuramae EK, van der Heijden MGA. 2019. Fungal-bacterial diversity and microbiome complexity predict ecosystem functioning. Nat Commun 10: 4841. https://doi.org/10.1038/s41467-019-12798-y.

Wang H, Yang Y, Yao C, Feng Y, Wang H, Kong Y, Riez U, uz Zaman Q, Fahad S, Deng G. 2024. The correct combination and balance of macronutrients nitrogen, phosphorus, and potassium promote plant yield and quality through enzymatic and antioxidant activities in potato. J Plant Growth Regul 43: 4716-4734. https://doi.org/10.1007/s00344-024-11428-2.

Wang X, Wang X, Sheng H, Wang X, Zhao H, Feng K. 2022. Excessive nitrogen fertilizer application causes rapid degradation of greenhouse soil in China. Pol J Environ Stud 31: 1527-1534. https://doi.org/10.15244/pjoes/143293.

Xiao Z, Zhang S, Yan P, Huo J, Aurangzeib M. 2022. Microbial community and their potential functions after natural vegetation restoration in gullies of farmland in Mollisols of Northeast China. Land 11 (12): 2231. https://doi.org/10.3390/land11122231.

Xing Y, Xie Y, Wang X. 2025. Enhancing soil health through balanced fertilization: A pathway to sustainable agriculture and food security. Front Microbiol 16: 1536524. https://doi.org/10.3389/fmicb.2025.1536524.

Xiong M, Wu H, Li J. Wan H, Chen X, Liu B, He J. 2025. *Terrimonas alba* sp. nov., an ochratoxin a degrading strain isolated from Lakeside Soil. Curr Microbiol 82: 269. https://doi.org/10.1007/s00284-025-04254-6.

Xu Y, Li H, Tan L, Li Q, Liu W, Zhang C, Gao Y, Wei X, Gong Q, Zheng X. 2022. What role does organic fertilizer actually play in the fate of antibiotic resistome and pathogenic bacteria in planting soil? J Environ Manag 317: 115382. https://doi.org/10.1016/j.jenvman.2022.115382.

Yadav R, Walia SS, Dheri GS, Singh G, Sharma K. 2024. Balanced fertilization through integrated nutrient management improves soil health, productivity, and profitability in potato-maize (fodder)-maize

system under Inceptisols of Indian subtropics. J Soil Sci Plant Nutr 25: 3881-3900. https://doi.org/10.1007/s42729-025-02372-5.

Yin S, Suo F, Zheng Y, You X, Li H, Wang J, Zhang C, Li Y, Cheng Y. 2022. Biochar-compost amendment enhanced sorghum growth and yield by improving soil physicochemical properties and shifting the soil bacterial community in a coastal soil. Front Environ Sci 10: 1036837. https://doi.org/10.3389/fenvs.2022.1036837.

Yu L, Li D, Zhang Y, Wang Y, Yao Q and Yang K. 2024. An optimal combined slow-release nitrogen fertilizer and urea can enhance the decomposition rate of straw and the yield of maize by improving soil bacterial community and structure under full straw returning system. Front Microbiol 15:1358582. https://doi: 10.3389/fmicb.2024.13585.

Zhang Y, Shen H, He X, Thomas BW, Lupwayi NZ, Hao X, Thomas MC, Shi X. 2017. Fertilization shapes bacterial community structure by alteration of soil pH. Front Microbiol 8: 1325. https://doi.org/10.3389/fmicb.2017.01325.

Zhou Z, Wu H, Li D, Zeng W, Huang J, Wu Z. 2022. Comparison of gut microbiome in the Chinese mud snail (*Cipangopaludina chinensis*) and the invasive golden apple snail (*Pomacea canaliculata*). PeerJ 5 (10): e13245. https://doi.org/10.7717/peerj.13245.